Koopman Operator Based Predictive Control With a Data Archive of Observables

Kartik Loya * **Jake Buzhardt** * **Phanindra Tallapragada** *

* *Department of Mechanical Engineering, Clemson University, Clemson, SC 29634 USA (e-mail: kloya@g.clemson.edu, jbuzhar@g.clemson.edu, ptallap@clemson.edu).*

Abstract:
The problem of control of complex system such as autonomous swimming robots, off-road vehicles, wind turbines and wind farms, transportation and power networks is often challenging due to high dimensional nonlinear models, unmodeled phenomena and parameter uncertainty. The increasing ubiquity of sensors and data measuring such systems, combined with increased computational resources has led to an interest in purely data driven control methods, in particular using the Koopman operator. In this paper we elucidate the construction of a linear predictor based on a sequence of time realizations of observables drawn from a data archive of different trajectories and combined with subspace identification methods for linear systems. This approach is free of any finite basis functions, but instead depends on the time realization of these basis functions. The improved prediction and control is demonstrated with examples. We further show that the basis functions can be constructed using time delayed coordinates of the outputs enabling the application to purely data driven systems.

Keywords: Koopman operator, Data Driven Control, Subspace Identification

1. INTRODUCTION

The problem of control of complex systems such as autonomous swimming robots, off-road vehicles, wind turbines and wind farms, transportation and power networks is often challenging due to high dimensional nonlinear models, unmodeled phenomena, and parametric uncertainty. The increasing ubiquity of sensors has led to an abundance of data from such systems, which combined with improved computational resources has led to an interest in purely data driven methods for modeling, analysis, and control of such systems Rowley et al. (2009); Susuki and Mezić (2014); Hou and Wang (2013). These data driven approaches have increasingly been based on linear operators associated with nonlinear dynamical systems. The Perron-Frobenius operator propagates the densities in the state space of a dynamical system and the Koopman operator propagates the observables along the flow in the state space of a dynamical system, see for example Lasota and Mackey (1994). By considering the evolution of functions of the states rather than the states themselves, these operator-based methods transform a nonlinear system into an infinite dimensional linear system, which can be approximated by a finite dimensional linear system such as in Williams et al. (2015); Klus et al. (2015). Additionally, many efforts have been made recently to extend these results from autonomous dynamical systems to input-output systems, where the operator approximation must account for the effect of a control input to predict the output variables. For example, extended dynamic mode decomposition (EDMD) coupled with model predictive control (MPC) such as in Korda and Mezic (2018) or with linear parameter varying (LPV) modes such as in Williams et al. (2016) and variations thereof have become popular. More recently ideas from subspace identification (SSID) for linear systems, such as from Ljung (1998) and Overschee and De Moor (1996) have been used by Lian and Jones (2019, 2020) to develop a method based on identifying the significant modes in the evolution of an observable along a single trajectory and then using Gaussian processes as a mapping to this identified lifted state. The current paper builds on these ideas of subspace identification and clarifies and extends them to include observation data from multiple trajectories and further shows that basis functions for the observables can be defined using only data from output variables.

The main contributions of the paper are as follows. We demonstrate the relation between a Koopman operator associated with a nonlinear system and subspace identification methods of linear systems. We identify the relation between the approximate Koopman operator that is calculated using techniques like EDMD versus subspace methods. In the approach using subspace methods, the approximate Koopman operator that is calculated propagates time realizations of observables. Therefore output data from a single trajectory does not (usually) sample the state space dynamics, as it is difficult to ensure that a nonlinear system is sufficiently excited, an assumption which underlies the subspace identification methods with

⋆ This work was supported by grant 2021612 from the National Science Foundation and grant 13204704 from the Office of Naval Research.

a single data record, see for example Willems et al. (2005). We show that using multiple data records improves the accuracy of prediction. Multiple data records have been shown to be useful even in subspace identification for linear systems in Holcomb and Bitmead (2017) since a sufficiently long single data record may not be available in practice and more importantly. The observables could be projected on any set of basis functions, such as Gaussian processes. Usually the basis functions are functions of the state and in purely data driven systems, such function cannot be constructed since explicit knowledge of the states is not available nor different observables realized or sampled. We show in this paper that the basis functions can be constructed using time delayed coordinates of the outputs enabling the application to purely data driven systems.

The rest of the paper is organized as follows. In section 2 we describe the approximations of the different 'versions' of the Koopman operator and in particular the approximation that propagates time realizations of the observables. In section 3 we formulate the subspace identification problem for the linearized dynamics using multiple data records; in 4 we review Gaussian processes (GP) as basis functions (of state variable) for observables and in 4.2 we reformulate the GP as basis functions of time delayed observables and demonstrate numerical results in 6.

2. FORMULATION FOR KOOPMAN OPERATOR BASED CONTROL

Consider the autonomous dynamical system defined on a manifold $\mathcal{M}$

$$\dot{x} = f(x) \tag{1}$$

with $f : \mathcal{M} \mapsto T_x\mathcal{M}$ and suppose the bounded function $g : \mathcal{M} \mapsto \mathbb{R}$ is an observable. The flow map of the dynamical system, $F_t : \mathcal{M} \mapsto \mathcal{M}$ propagates the state as $x(t + t_0) = F_t(x(t_0))$. The Koopman operator $\mathcal{K} : \mathcal{L}^\infty \mapsto \mathcal{L}^\infty$ propagates the observable as $\mathcal{K}g(x(t_0)) = g \circ F_t(x(t_0)))$. For the discrete time dynamical system

$$x_{t+1} = F(x_t) \tag{2}$$

where $x_t \in \mathcal{M}$ and $F : \mathcal{M} \mapsto \mathcal{M}$, the action of the Koopman operator on an observable function $g : \mathcal{M} \mapsto \mathbb{R}$ is given as follows.

$$\mathcal{K}g(x_t) = (g \circ F)(x_t) = g(x_{t+1}). \tag{3}$$

In practice, the action of the infinite dimensional Koopman operator is approximated by its action on a finite dimensional space, called the lifted space. This has frequently been done through by projection to a finite set of basis functions called the dictionary Williams et al. (2015); Korda and Mezic (2018) that can either be defined a priori or learned as part of the system identification procedure or through the use of neural networks such as in Li et al. (2017); Lusch et al. (2018). Here we take a different approach and treat the sequence of measurements $y_t \in \mathbb{R}^p$ as evaluations of an observable function of the state. This observable function is treated as a linear combination of a finite basis functions $\Psi(x_t)$ which would be propagated by an approximation of the Koopman operator K_Ψ

$$\mathcal{K}g(x_t) \approx \mathcal{K}[c^\intercal \Psi](x_t) \approx (K_\Psi c)^\intercal \Psi(x_t) \tag{4}$$

as shown in Fig. 1. Here c is a vector of projection coefficients for the projection of g onto the function space spanned by the dictionary functions Ψ. In order to obtain

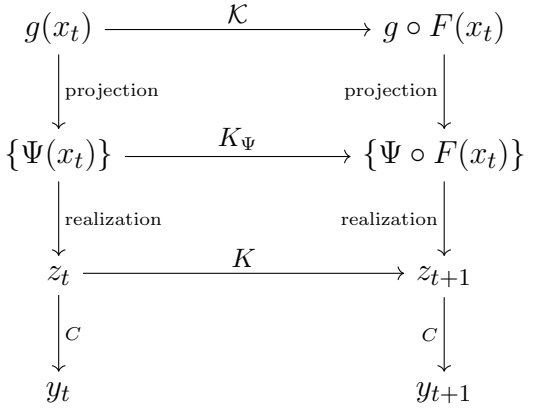

Fig. 1. Commutative diagram showing the propagation of the observable $g(x)$ by the operator $\mathcal{K}$, the propagation of the projected observables $\Psi(x)$ by the projected operator K_Ψ and their time realization z_t by the operator K.

an appropriate set of dictionary functions, Ψ, we first obtain a lifted state z_t and a corresponding operator K, which propagates it forward in time by applying ideas of subspace identification using temporal sequences of data without first approximating the operator K_Ψ or specifying the basis functions Ψ. These lifted states z_t are then regarded as evaluations at a particular x_t of a realization of a random variable in a function space. This notion of a random variable in a function space allows us to apply Gaussian process regression (see Rasmussen and Williams (2006)), which can be viewed as obtaining an a posteriori distribution in a function space, conditioned on the given data. That is, we model the lifted states as a Gaussian process

$$z_t \sim \Psi(x_t) = \mathcal{GP}(\mu(x_t), k(x_t, x_t)). \tag{5}$$

Further, if we only have access to an output measurement, y_t which can be regarded as a function of the state x_t, the same lifting procedure can be applied to y_t, as this can be interpreted as indirectly lifting the state x_t. The measurements y_t can then be retrieved as a projection by the operator C from the lifted space of realized observables. This matrix C is also obtained through the subspace identification procedure, but in the Koopman interpretation, its rows contain the projection coefficients c from Eq. (4) corresponding to the particular observable functions associated with the output measurements y_t. In this interpretation a Koopman operator can be constructed that propagates the observables as functions of time without first specifying or learning a dictionary of basis functions.

The formulation can be extended to a control system on realizations of observables $z(t)$ with a control input at time t as $u_t \in \mathbb{R}^m$

$$z_{t+1} = Kz_t + Bu_t \tag{6a}$$

$$y_t = Cz_t + Du_t \tag{6b}$$

3. KOOPMAN OPERATOR VIA OBSERVABLES FROM MULTIPLE DATA RECORDS

We begin by collecting a dataset of input-output data from N trajectories of $n + 1$ timesteps each, $\mathcal{D}_i = \{u_t^i, y_t^i\}_{t=0}^n$

for $i = 1, \ldots, N$. We define the Hankel matrices for each trajectory of $n+1$ measured output and input data and with l time delayed coordinates as,

$$Y_l^i = \begin{pmatrix} y_0^i & y_1^i & \cdots & y_{n-l}^i \\ y_1^i & y_2^i & \cdots & y_{n-l+1}^i \\ \vdots & \vdots & \ddots & \vdots \\ y_{l-1}^i & y_l^i & \cdots & y_n^i \end{pmatrix} U_l^i = \begin{pmatrix} u_0^i & u_1^i & \cdots & u_{n-l}^i \\ u_1^i & u_2^i & \cdots & u_{n-l+1}^i \\ \vdots & \vdots & \ddots & \vdots \\ u_{l-1}^i & u_l^i & \cdots & u_n^i \end{pmatrix}$$

In order to identify the system using the multiple trajectory records, these Hankel matrices are collected to form mosaic-Hankel matrices van Waarde et al. (2020) as shown below

$$Y_l = \begin{bmatrix} Y_l^1 & Y_l^2 & \cdots & Y_l^N \end{bmatrix}, \qquad U_l = \begin{bmatrix} U_l^1 & U_l^2 & \cdots & U_l^N \end{bmatrix}$$

where, $Y_l \in \mathbb{R}^{lp \times (n-l)N}$ and $U_l \in \mathbb{R}^{lm \times (n-l)N}$.

3.1 System matrix calculation using SSID

Assuming that we have collected the trajectory data and organized it into a mosaic Hankel matrix as mentioned above, we proceed by computing the lifted states Z_0^{lift} and system matrices K, C, B, and D using an SSID algorithm for multiple trajectories. We outline the procedure below, following closely the presentation of Holcomb and Bitmead (2017). The system (6) can be concatenated and represented in the form as,

$$Y_l = \Gamma_l Z_0^{\text{lift}} + \mathcal{H}_l U_l \tag{7}$$

where

$$\Gamma_l = \begin{bmatrix} C \\ CK \\ CK^2 \\ \vdots \\ CK^{l-1} \end{bmatrix}, \quad \mathcal{H}_l = \begin{bmatrix} D & 0 & 0 & \cdots & 0 \\ CB & D & 0 & \cdots & 0 \\ CKB & CB & D & \cdots & 0 \\ \vdots & \vdots & \vdots & \ddots & \vdots \\ CK^{l-2}B & \cdot & \cdot & \cdots & D \end{bmatrix}$$

$$Z_0^{\text{lift}} = \begin{bmatrix} z_0^1 \cdots z_{n-l}^1 & z_0^2 & \cdots & \cdots & z_{n-l}^{N-1} & z_0^N \cdots z_{n-l}^N \end{bmatrix}$$

Where $\Gamma_l \in \mathbb{R}^{lp \times N}$ is the extended observability matrix, $\mathcal{H}_l \in \mathbb{R}^{lp \times lm}$ is the block-Toeplitz matrix and $Z_0^{\text{lift}} \in \mathbb{R}^{l \times (n-l)N}$ is the matrix of lifted states for the initial state of each trajectory. The subspace system identification algorithm proceeds by projecting Eq. (7) onto the orthgonal complement of the rowspace of U_l. The projection operator for this is given by $\Pi_{U_l}^{\perp} = I - U_l^{\intercal}(U_l U_l)^{\dagger} U_l$ and this projection yields $Y_l \Pi_{U_l}^{\perp} = \Gamma_l Z_0^{\text{lift}} \Pi_{U_l}^{\perp}$. With this, we extract column space of Γ_l by taking the singular value decomposition of $Y_n \Pi_{U_n}^{\perp}$

$$Y_n \Pi_{U_n}^{\perp} = [Q_1 \, Q_2] \begin{bmatrix} \Sigma_1 & 0 \\ 0 & \Sigma_2 \end{bmatrix} \begin{bmatrix} V_1^{\intercal} \\ V_2^{\intercal} \end{bmatrix}$$

where Σ_1 contains the r largest singular values, and so we consider an approximation of Γ_l to be $\hat{\Gamma}_r = Q_1 \Sigma_1^{\frac{1}{2}}$. By selecting the r largest singular values we are determining the order of the lifted dynamics. Therefore, the first p rows of $\hat{\Gamma}_r$ give us the C matrix

$$C = \hat{\Gamma}_r(1:p, :) \tag{8}$$

and with this, the K matrix can be found by solving the following least squares problem

$$K = [\hat{\Gamma}_r(1:(n-1)p, :)]^{\dagger} \, \hat{\Gamma}_r(p+1:np, :) \tag{9}$$

where the : operator is used as in the familiar MATLAB syntax and $(\cdot)^{\dagger}$ is the Moore-Penrose pseudoinverse.

We again form a least squares problem to find matrices B, D and, Z_0^{lift}, using the equation below where $i = 1, 2, \ldots, N$ and $t = 0, 1, 2, \ldots, l$.

$$y_t^i = CK^t z_0^i + \sum_{k=1}^{t} CK^{(t-k)} B u_{k-1}^i + D u_t^i$$

We first vectorize and collect all outputs in one vector and write it in the form,

$$\begin{aligned} vec(Y) &= \begin{bmatrix} y_0^1 \cdots y_n^1 & y_0^2 \cdots \cdots y_n^{N-1} & y_0^N \cdots y_n^N \end{bmatrix}^{\intercal} \\ &= \begin{bmatrix} \Phi_B^{\intercal} & \Phi_D^{\intercal} & \Phi_{Z_0^{\text{lift}}}^{\intercal} \end{bmatrix} \begin{bmatrix} vec(B)^{\intercal} & vec(D)^{\intercal} & Z_0^{\text{lift}\intercal} \end{bmatrix}^{\intercal} \\ &= \Phi^{\intercal} \theta \end{aligned}$$

With this, the matrices B, D and the initial lifted state Z_0^{lift} are given by the least square solution

$$\hat{\theta} = \begin{bmatrix} vec(B) \\ vec(D) \\ \hat{Z}_0^{\text{lift}} \end{bmatrix} = (\Phi \Phi^{\intercal})^{-1} \Phi \; vec(Y)$$

4. GAUSSIAN PROCESSES AS BASIS FUNCTIONS

The SSID procedure outlined in the previous section for identifying the lifted state z and system matrices provides a method for obtaining the system matrices from input-output data collected from the system. However, it is also necessary to construct a mapping from the original states, x_t (or partial observation y_t) to the lifted state. For this, we employ Gaussian process regression, based on the idea discussed in Sec. 2 that the lifted states z_t obtained in subspace identification can be viewed as evaluations at a particular x_t of a dictionary function, which is itself a realization of a random variable in a function space. In Sec. 4.1 we give the procedure when measurements of the full state observable are available and in Sec. 4.2 we consider the case where only a partial observation is available.

4.1 Gaussian Processes as Basis functions of full state observable

The purpose of the Gaussian process model here is to give the mapping $z_t = \Psi(x_t)$ from the original system states $x \in \mathbb{R}^d$ to the lifted states $z \in \mathbb{R}^r$.

For this, we use the data gathered above as Z_0^{lift} and corresponding states $X = [x_0^1, \cdots, x_{n-l}^1, \cdots, x_0^N, \cdots, x_{n-l}^N]$ obtained from the first p rows of the mosaic-Hankel matrix Y_l for the case when we have full state observable that is $y_t = x_t$. This data is then used to model each lifted state as a Gaussian process.

$$z_i(x) | \mathcal{D} \sim \mathcal{GP}(\mu_{z_i|\mathcal{D}}(x), k_{z_i|\mathcal{D}}(x, x)) \tag{10}$$

where $i = 1, 2, \cdots, r$. The posterior mean and covariance are calculated as

$$\mu_{z_i|\mathcal{D}}(x) = \mu(x) + K_{xX} \left(K_{XX} + \sigma_n^2 I \right)^{-1} Z_0^{\text{lift}}(i, :)^{\intercal} \tag{11}$$

$$k_{z_i|\mathcal{D}}(x, x) = K_{xx} - K_{xX} \left(K_{XX} + \sigma_n^2 I \right)^{-1} K_{Xx} \tag{12}$$

where the kernel matrices are found by evaluating the kernel function. In particular, we are using the ARD squared exponential kernel. The kernel parameters can be optimized through log-likelihood maximization. Here this is done using the MATLAB toolbox for Gaussian process regression to fit each of the r GPs independently.

4.2 Gaussian Processes as Basis functions of time delayed observables

Often in system identification theory Ljung (1998), using time-delayed state observables to identify the whole nonlinear states can be an effective way to estimate the state of a system even if the full state is not directly measured. Therefore, when the output is not a full state, the Gaussian process model gives the mapping from the output and the time-delayed coordinates of outputs and inputs to the lifted states $z_t = \Psi(\hat{x})$.

$$\begin{aligned}\hat{x}_t &= [y_t, y_{t-1}, \cdots, y_{t-k}, u_{t-1}, \cdots, u_{t-k}]^\intercal \\ \hat{X} &= [\hat{x}_0^1, \cdots, \hat{x}_{n-l}^1, \cdots, \hat{x}_0^N, \cdots, \hat{x}_{n-l}^N]\end{aligned} \tag{13}$$

These time-delayed observables $\hat{X}$ with the corresponding realizations of the lifted state Z_0^{lift} is used to model the lifted state as Gaussian process.

$$z_i(\hat{x})|\mathcal{D} \sim \mathcal{GP}(\mu_{z_i|\mathcal{D}}(\hat{x}), k_{z_i|\mathcal{D}}(\hat{x}, \hat{x})) \tag{14}$$

The posterior mean and covariance are calculated using (11) and (12).

5. PREDICTION USING GP-SSID

For predicting the evolution of the system from a given initial condition x_0, the initial condition of the lifted state is represented as a Gaussian random variable, found by evaluating the GP at x_0.

$$z_0 \sim \mathcal{GP}(\mu_{z|\mathcal{D}}(x_0),\, k_{z|\mathcal{D}}(x_0, x_0)) \tag{15}$$

That is, the mean and covariance of the initial lifted state are found by evaluating the posterior mean and covariance for each lifting function, using (11) and (12).

$$\mu_{z|\mathcal{D}}(x_0) = \begin{bmatrix}\mu_{z_1|\mathcal{D}}(x_0) & \cdots & \mu_{z_r|D}(x_0)\end{bmatrix}^\intercal \tag{16a}$$

$$k_{z|\mathcal{D}}(x_0, x_0) = \text{diag}\begin{bmatrix}k_{z_1|\mathcal{D}}(x_0, x_0) & \cdots & k_{z_r|D}(x_0, x_0)\end{bmatrix} \tag{16b}$$

Then, denote the mean and covariance of the lifted state by $\bar{z} = \mu_{z|\mathcal{D}}$ and $P = k_{z|\mathcal{D}}$, respectively. This mean and covariance are propagated forward in time using the system matrices as

$$\bar{z}_{t+1} = K\bar{z}_t + Bu_t \tag{17a}$$

$$P_{t+1} = KP_tK^\intercal \tag{17b}$$

and the estimated mean of the output, $\hat{y}$ along with its covariance Q at each step can be obtained as

$$\hat{y}_t = C\hat{z}_t + Du_t \tag{18a}$$

$$Q_t = C\,P_t\,C^\intercal \tag{18b}$$

where t is the time index.

6. RESULTS

6.1 Linear predictor without Control

We apply the proposed method to obtain the Koopman operator for the nonlinear Duffing oscillator using multiple and single data records. Then, we compare the open-loop prediction of each linear model against the true trajectory simulated using the nonlinear model,

$$\begin{aligned}\dot{x}_1 &= x_2 \\ \dot{x}_2 &= 4x_1 - x_1^3 \\ y &= \begin{bmatrix}x_1 & x_2\end{bmatrix}^\intercal\end{aligned} \tag{19}$$

The training data set is collected by discretizing the nonlinear system (19) using a fourth order Runge-Kutta method and time step 0.01s. For the first linear model (multiple data records), we sample 200 trajectories all randomly initialized for $x \in \mathbb{R}^2$ in the range $[-3, 3]$ and simulate each trajectory for 150-time steps. We then con-

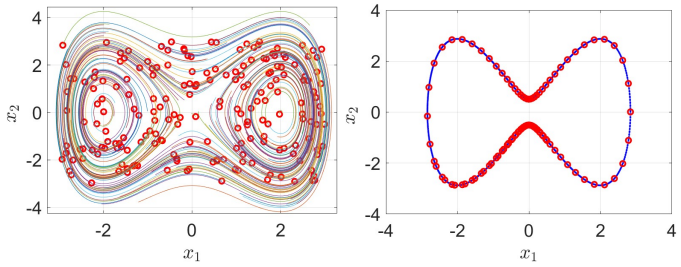

Fig. 2. (a) training data set for the model with multiple data records (b) training data for the single trajectorycase. Red points are the training data for the GP and multicolored lines show the full trajectories.

struct the mosaic-Hankel matrix and follow the procedure discussed in section 3 to construct a higher dimensional linear system. For the second model, we sample a single trajectory of 8000 time steps long and use this data again to construct the Koopman operator for the duffing oscillator. We select 200 data points and the corresponding

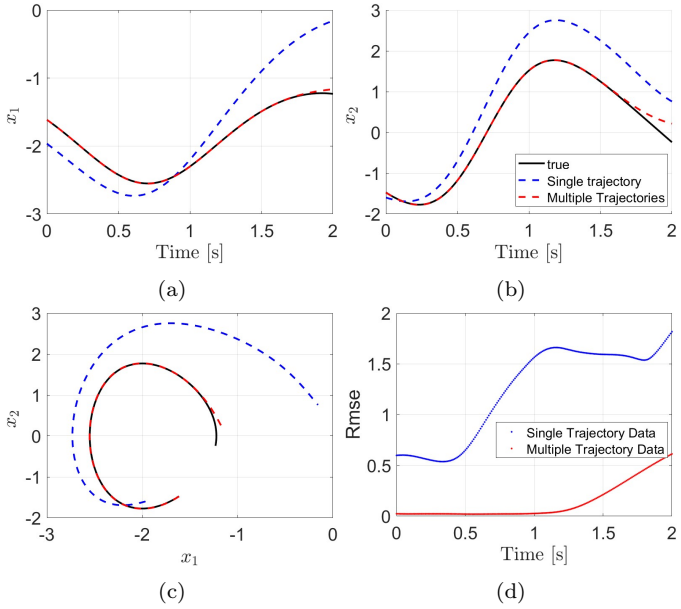

Fig. 3. Comparing the prediction of multiple trajectory model and single trajectory model with the nonlinear system (19) for the initial state [0.4037,-1.7912].

time realization of the basis functions (Z_{lift}) from both models, which we use to train the Gaussian processes. In the case of the multiple trajectory model, we select $r = 10$, while for the single trajectory model, we select $r = 20$. For predicting the forward dynamics we first use the respective trained Gaussian processes to lift the initial states to the lifted space and then propagate forward using (17) and (18).

We generated 500 randomly sampled points in the state space to test both models and predicted a 2-second tra-

jectory for each. The root means squared error for the model trained with multiple trajectories is 0.0534, while for the single trajectory model, it is 0.5186. Figure 3(a-c) shows one of the prediction example with an initial state at $[0.4037, -1.7912]$. Figure 3d illustrates the increase in RMSE as we predict further into the future.

6.2 MPC with Koopman operator

In this section, we consider a Duffing oscillator with a control input

$$\begin{aligned} \dot{x}_1 &= x_2 \\ \dot{x}_2 &= -0.2x_2 + 4x_1 - x_1^3 + u \\ y &= [x_1 \quad x_2]^\intercal \end{aligned} \tag{20}$$

For comparison purposes, we identify two linear models, one based on multiple data records and the other on a single trajectory. Next we use linear model predictive control (MPC) technique to control the nonlinear system (20) and compare these two linear models in terms of the performance index of the MPC and convergence to the desired output.

We gather a training data set for the first model using multiple data records by simulating 100 randomly sampled initial states forward for 400-time steps with random control inputs $u \in [-3, 3]$. For the second model, we propagate an initial condition for 8000-time steps with a random control input of a similar range. Subsequently,

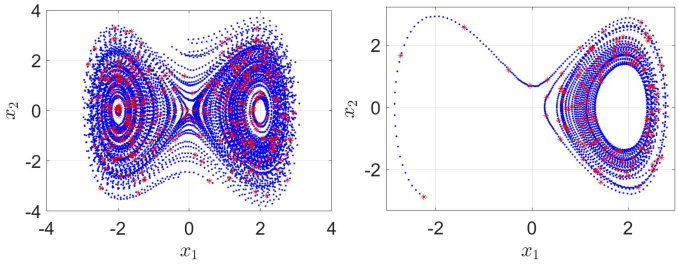

Fig. 4. Training data set for the Duffing oscillator (20). Red points are the training data for the GPs, and the blue points show the full trajectories. (a) multiple data records, (b) single trajectory

we construct mosaic-Hankel matrices from the collected data, identify the linear system matrices, and train the basis function (Gaussian Processes) for both models, as discussed in sections 3 and 4. The size of the lifted states selected is $r = 35$ for the model based on multiple data records and $r = 30$ for the model using single trajectory data.

Linear model predictive control (MPC) techniques is utilized with the identified linear models to guide the system's states toward a desired state/trajectory. MPC optimizes the performance of dynamic systems by solving a sequence of optimization problems, determining the best control inputs that minimize the deviation between the desired and actual outputs while ensuring compliance with imposed constraints. We can formulate the MPC as a quadratic optimization problem with constraints as

$$\min_u \sum_{j=t_i}^{t_i+N_p} \frac{1}{2}\Big((y_j - y_j^r)^\intercal Q_j (y_j - y_j^r) + u_j^\intercal R_j u_j\Big) \tag{21}$$

$$\begin{aligned} \text{s.t.} \quad & Z_0 = \mathcal{GP}(\mu(x_0), k(x_0, x_0)) \\ & Z_{j+1} = KZ_j + Bu_j, \qquad j = t_i. \ldots . N_p \\ & y_j = CZ_j \\ & u_{min} \le u_j \le u_{max} \end{aligned}$$

Where $Q_j = 10$, $Q_{N_p} = 20$ and $R_j = 0.01$ are the positive semi-definite weight matrices for the outputs and inputs, t_i is the current time, $N_p = 100$ is the prediction horizon and y^r is the reference trajectory that is to be tracked. In this example, we want to drive a given initial state x_0

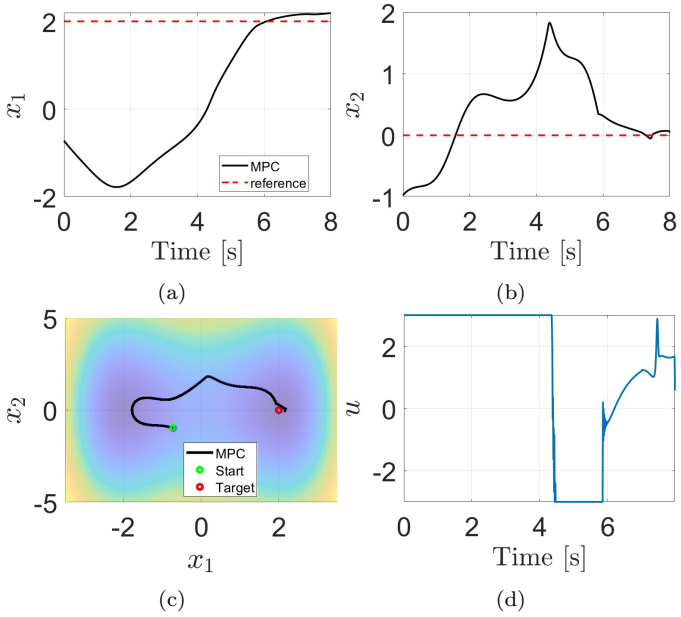

Fig. 5. MPC results for linear model constructed using multiple data records. The initial state $x_0 = [-0.7160, -0.9789]$ and the target state is $[2, 0]$. In (c), color indicates the total energy level.

to a desired state $x_{des} = [2, 0]$. At the start of the MPC, the Gaussian processes are used to lift the initial state x_0. Then MPC predicts for N_p-time step, and one control step is implemented, which updates the initial state. Each of these feedback updates are passed again through the Gaussian process, and the process continues. Figure 5 shows the results for the first model, which uses multiple data records, and in figure 6 are the results for the model using single trajectory data.

6.3 MPC with Koopman operator for partially observed state

Consider the Duffing oscillator with control in (20), which is partially observed such that

$$y = x_2 \tag{22}$$

Collecting data and identifying the Koopman operator using subspace identification remains similar to the previous example in section 6.2. We sample 100 trajectories with random initial states propagated for 400-time steps with random control inputs. To train the basis function (Gaussian processes), we use output y along with 5 time-delayed inputs and outputs with the corresponding time

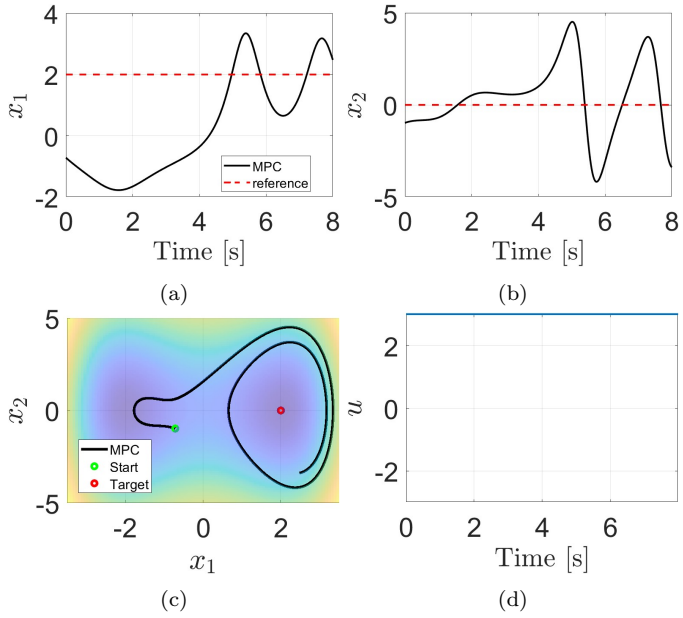

Fig. 6. MPC results for linear model constructed using single trajectory data. The initial state $x_0 = [-0.7160, -0.9789]$ and the target state is $[2, 0]$. In (c), color indicates the total energy level.

realizations of the lifted function $Z_{\text{lift}} \in \mathbb{R}^{25}$. We formulate a similar MPC model (21) as discussed in the previous section to control the output x_2 to stabilize at 0. Here, the weight matrices used are $Q_j = 100$ and $R_j = 0.001$.

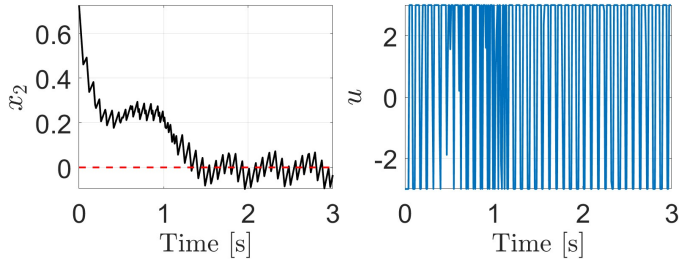

Fig. 7. MPC result for tracking the observable x_2 to 0.

7. CONCLUSION

In this paper we have explored connections between the classical system identification technique of subspace identification and recently developed methods for system identification based on constructing a finite dimensional approximation of the Koopman operator. In particular, we have shown that these methods can be directly related by considering the latent state identified through SSID to be an evaluation of a set of dictionary functions at a particular state of the underlying nonlinear system. With this formulation, we have shown that for nonlinear systems, it is necessary to consider multiple data records, as a single trajectory does not sufficiently explore the state space in most cases. This is indicated by improved prediction and control performance. We also show that the same formulation can be applied in cases where only partial state measurements are available.

REFERENCES

Holcomb, C.M. and Bitmead, R.R. (2017). Subspace identification with multiple data records: unlocking the archive. *arXiv preprint arXiv:1704.02635*.

Hou, Z.S. and Wang, Z. (2013). From model-based control to data-driven control: Survey, classification and perspective. *Information Sciences*, 235, 3–35.

Klus, S., Koltai, P., and Schütte, C. (2015). On the numerical approximation of the Perron-Frobenius and Koopman operator. *arXiv preprint arXiv:1512.05997*.

Korda, M. and Mezic, I. (2018). Linear predictors for nonlinear dynamical systems: Koopman operator meets model predictive control. *Automatica*, 149–160.

Lasota, A. and Mackey, M.C. (1994). *Chaos, Fractals, and Noise : Stochastic Aspects of Dynamics*. Springer.

Li, Q., Deitrich, F., Bollt, E.M., and Kevrekidis, I.G. (2017). Extended dynamic mode decomposition with dictionary learning: A data-driven adaptive spectral decomposition of the Koopman operator. *CHAOS*, 27, 103111.

Lian, Y. and Jones, C.N. (2019). Learning feature maps of the koopman operator: A subspace viewpoint. In *2019 IEEE 58th Conference on Decision and Control (CDC)*, 860–866.

Lian, Y. and Jones, C.N. (2020). On gaussian process based koopman operators. *IFAC-PapersOnLine*, 53(2), 449–455.

Ljung, L. (1998). *System identification*. Springer.

Lusch, B., Kutz, J.N., and Brunton, S.L. (2018). Deep learning for universal linear embeddings of nonlinear dynamics. *Nature communications*, 9(1), 4950.

Overschee, P. and De Moor, B. (1996). *Subspace Identification for Linear Systems*. Springer.

Rasmussen, C.E. and Williams, C.K.I. (2006). *Gaussian processes for machine learning*. Adaptive computation and machine learning. MIT Press, Cambridge, Mass. OCLC: ocm61285753.

Rowley, C.W., Mezic, I., Bagheri, S., Schlatter, P., and Henningson, D.S. (2009). Spectral analysis of nonlinear flows. *Journal of Fluid Mechanics*, 641, 115–127.

Susuki, Y. and Mezić, I. (2014). Nonlinear koopman modes and power system stability assessment without models. *IEEE Transactions on Power Systems*, 29(2), 899–907.

van Waarde, H.J., De Persis, C., Camlibel, M.K., and Tesi, P. (2020). Willems' Fundamental Lemma for State-Space Systems and Its Extension to Multiple Datasets. *IEEE Control Systems Letters*, 4(3), 602–607.

Willems, J.C., Rapisarda, P., Markovsky, I., and De Moor, B.L. (2005). A note on persistency of excitation. *Systems & Control Letters*, 54(4), 325–329.

Williams, M.O., Hemati, M.S., Dawson, S.T., Kevrekidis, I.G., and Rowley, C.W. (2016). Extending data-driven koopman analysis to actuated systems. *IFAC-PapersOnLine*, 49(18), 704–709.

Williams, M.O., Kevrekidis, I.G., and Rowley, C.W. (2015). A data–driven approximation of the Koopman operator: Extending dynamic mode decomposition. *Journal of Nonlinear Science*, 25(6), 1307–1346.